Microfluidic Production of Cell-Laden

Microspheroidal Hydrogels with Different

Geometric Shapes

Yuan Tian, Elizabeth A. Lipke*

212 Ross Hall, Auburn University, AL, 36849

Corresponding Author

*Email: elipke@auburn.edu.

KEYWORDS: Microspheroid, tissue engineering, microsphere, microrod, anisotropy, T-junction

ABSTRACT

Providing control over the geometric shape of cell-laden hydrogel microspheroids, such as

diameter and axial ratio, is critical for their use in biomedical applications. Building on our

previous work establishing a microfluidic platform for production of large cell-laden microspheres,

here we establish the ability to produce microspheroids with varying axial ratio (microrods) and

elucidate the mechanisms controlling microspheroidal geometry. Microspheroids with radial

diameters ranging from 300 to over 1000 µm and axial ratios from 1.3 to 3.6 were produced.

1

Although for microfluidic devices with small channel sizes (typically < 500 μm) the mechanisms governing geometric control have been investigated, these relationships were not directly translatable to production of larger microspheroids (radial diameter $10^2 - 10^3 \, \mu m$) in microfluidic devices with larger channel sizes (up to 1000 µm). In particular as channel size was increased, fluid density differences became more influential in geometric control. We found that two parameters, narrowing ratio (junction diameter over outlet diameter) and flow fraction (discrete phase flow rate over total flow rate), were critical in adjusting the capillary number, modulation of which has been previously shown to enable control over microspheroid diameter and axial ratio. By changing the device design and the experimental conditions, we exploited the relationship between these parameters to predictably modulate microspheroid geometric shape. Finally, we demonstrated the applicability to tissue engineering through encapsulation of fibroblasts and endothelial colony forming cells (ECFCs) in hydrogel microspheroids with different axial ratios and negligible loss of cell viability. This study advances microfluidic production of large cellladen microspheroids (microspheres and microrods) with controllable size and geometry, opening the door for further investigation of geometric shape-related biomedical applications such as engineered tissue formation.

Introduction

Hydrogel microparticles with controlled geometric shapes are widely used for applications in material design, drug delivery, and tissue engineering. The geometric shape, such as size and anisotropy, plays an important role in microparticle function. For tissue engineering, hydrogels are commonly used for cell encapsulation. Providing control over hydrogel geometry can influence a range of microparticle properties from their injectability to self-assembly. Therefore, being able to produce hydrogels with different function-related shapes are beneficial for various applications such as cell delivery, bioreactor-based cell production, high throughput screening, and macroscopic tissue assembling. For example, microspherical hydrogels are widely used for injectable cell delivery, and properly controlled sizes can improve cell retention while allowing for a smooth injection process. Towards that end, significant attention has been paid to establishing an understanding of systematic modulation of microparticle geometry for production processes.

A number of techniques have been developed to produce hydrogels with different geometric shapes; these can be categorized as either batch production or continuous production. Two major types of batch process techniques, molding and photolithography, allow for the production of hydrogel microparticles with various shapes and a wide range of sizes (from submicron to millimeter scale).³ Whereas these two techniques provide a high degree of control over the hydrogel geometry, they have low production rates, severely limiting their commercial use. Another method widely used for batch production of hydrogel microparticles is emulsification, during which aqueous droplets of hydrogel precursors are generated from agitating a multiphase

mixture. 12 While emulsification provides a straightforward production approach, the hydrogels are limited to spherical shape and have a wide size distribution.

Compared to batch processes, microfluidics provides a continuous production approach, which increases the production throughput. Microfluidic devices are usually fabricated either using poly(dimethyl siloxane) (PDMS) or through the assembly of capillaries. Particle production within the device can be achieved with either single phase or multiple phase fluids. For single phase microfluidics, the Doyle group reported a method using microscope projection photolithography through which exotic non-spherical shapes can be produced within microfluidic channels.¹³ When employing multiphase fluids, various junction designs have been introduced for geometric control, such as T-junction, flow-focusing, and co-flow designs. ¹⁴ The results have been used for numerous applications, including drug delivery, 15 functional macro- or super- molecule encapsulation, 16 and cell encapsulation.¹⁷ However, channel size in these devices typically has an upper limit (< 200 μm for PDMS devices and < 500 μm for capillary devices) and therefore results in constrained maximum hydrogel sizes (particularly radial diameters) and cell densities. 18-21 For this reason, exploration and examination of the mechanisms governing geometric control have been focused on small diameter particles (Figure 1A). Particles with larger radial diameters are also needed, however, in various commercial biomedical applications, especially in cell encapsulation. For instance, production of engineered tumor spheroids with high cell density and large sizes is important in creating hypoxia-induced necrosis for cancer drug testing.²² In looking to control the production process of these larger particles, findings for geometric control of particles produced in small microfluidic channels are not directly translatable. In particular, when channel size increases, the effects of buoyancy and gravity, which stem from the density difference between phases, become more significant compared with surface tension. Therefore, establishing a greater level of understanding that builds on previous work for geometric control with small microfluidic devices is essential for controlling larger dimension (radial diameter 10^2 - 10^3 µm) particle size and shape.

Previously, we reported a microfluidic platform that supports rapid production of hydrogel microspheroids with large sizes (radial diameter up to 1100 µm) and high cell density (up to 60 million cell/mL). However, the capacity of this platform for systematic control over geometry had yet to be investigated. In this study, we explore the ability of this platform to control hydrogel microparticle geometric shape and elucidate the fundamental principles governing this control for the modified T-junction design used in this microfluidic device. The authors hypothesized that the geometric shape of the microspheroids could be controlled by adjusting the relative effect of viscous force versus surface tension at the interface between the continuous phase and discrete phase. Since substantially changing the surface tension could negatively impact cell membrane integrity, this parameter needed to be kept relatively constant; therefore, modulation of this relationship focused on changing the viscous force, which is proportional to the interfacial flow velocity difference. In particular, we examined the relationship between the capillary number and device design parameters, such as junction to outlet diameter ratio, along with experimental parameters, such as continuous to discrete phase flow rate ratio. Additionally, because of the increased size of the microfluidic channels, the effect of buoyancy and gravity was anticipated to play an important role in microfluidic device operation, and the ability to exploit this effect on device operation was tested by changing the device orientation. Microspheroids were prepared with radial diameter ranging from 300 µm to 1000 µm and axial ratio (AR) ranging from 1 to 3.6. As a proof-of-concept, anisotropic cell-laden tissues were produced and used for assembly of macroscopic tissues to demonstrate the potential of the microfluidic encapsulation device in biomedical applications.

Experimental Section

Microspheroid Production Using Microfluidic Platform. A detailed description of materials, microfluidic device fabrication, and microfluidic platform setup can be found in the Supporting Information (S1-2). Briefly a polydimethylsiloxane (PDMS) microfluidic device was fabricated using a molding technique. Poly(ethylene glycol)-fibrinogen (PEG-fibrinogen) hydrogel precursor solution was prepared with photoinitiator Eosin Y. As previously reported, a microfluidic platform consisting of the microfluidic device, syringe pumps, and a light source was built.²³ Aqueous hydrogel precursor solution (the discrete phase) and mineral oil (the continuous phase) was pumped into the microfluidic device. Microspheroids were formed at the junction, photocrosslinked in the outlet channel, and collected at the end of the outlet channel. At the ambient temperature of 23°C, the densities for the acellular hydrogel precursor solution and mineral oil were 1.0 and 0.85 g/mL, and the dynamic viscosities were approximately 1.4 and 30 mPa·s.¹⁰

Microspheroid Geometry Characterization. The resulting hydrogel microspheroids, including microspheres and microrods, were imaged using an inverted Nikon Eclipse Ti microscope. Using ImageJ software (NIH), axial diameter and radial diameter of the microspheroids were determined. The Axial Ratio (AR) was calculated using the formula:

$$Axial\ Ratio = \frac{Axial\ diameter}{Radial\ diameter} \tag{1}$$

A higher AR value corresponds to a longer microrod, and a perfect microsphere has an AR value of 1. For clarification purposes, a microspheroid is named microsphere when its AR is smaller than 1.05, and axial diameter is reported as diameter in the text when the difference between axial and radial diameter is small (< 5%). Uniformity was analyzed by coefficient of variance (CV).

Cell Culture and Maintenance. BJ-5ta (ATCC® CRL4001TM) normal human foreskin immortalized fibroblasts were obtained from ATCC (Manassas, VA). The cells were cultured in media containing 70.6% (v/v) Dulbecco's Modified Eagle's Medium (DMEM; Gibco), 18% (v/v) Medium 199 (Gibco), 10% (v/v) fetal bovine serum (FBS; Atlanta Biologicals), 1.4% (v/v) glutaGRO (Corning), and 0.02% (v/v) hygromycin B (Millipore). The cells were maintained at 37°C with 5% CO₂. Cells cultured in tissue-culture flask were detached with TypLETM Express Enzyme (Gibco) and used for 3D encapsulation.

Equine endothelial colony forming cells (ECFCs) were isolated following a previously published method.²⁴ All procedures involving animals were approved by the Auburn University Animal Care and Use Committee. The cells were cultured in collagen-coated tissue culture flask containing 95% (v/v) EBMTM-2 Basal Medium (Lonza), 5% (v/v) horse serum (HyClone), and EGMTM-2 SingleQuotsTM Supplements (Lonza) at 37°C with 5% CO₂. Cells were detached with TypLETM Express Enzyme (Gibco) and used for 3D encapsulation.

Cell Viability Assay. Cell viability after encapsulation was assessed using Live/DeadTM Viability/Cytotoxicity Kit (Invitrogen). Cell-laden microspheroids were incubated with Calcein-AM and Ethidium Homodimer-1 for 30 minutes. Z-stack images were then taken with fluorescence microscope (Nikon Eclipse Ti). Three regions with same size (190×190 μm) were randomly

selected on each microspheroids using ImageJ, and live/dead cells were counted through the optical slices along the z-axis for approximately 350 µm.

Phalloidin Staining. Fibroblast-laden microspheroids were rinsed with PBS to remove media and fixed with 4% paraformaldehyde for 30 minutes at room temperature. They were subsequently rinsed with PBS and stained with Alexa Fluor 568 Phalloidin for 1 hour. After washing with PBS, fluorescence images were obtained using confocal microscopy (Nikon AI Confocal Scanning Laser Microscope).

Statistical Analysis. All data are presented as mean ± standard deviation. All statistical analysis was performed using Minitab 18 Statistical Software (Minitab Inc.). After checking for normality of distribution, one-way analysis of variance (ANOVA) followed by Tukey-Kramer honest significant difference (HSD) test was performed to evaluate statistical significance between multiple groups. Statistical significance was declared if p<0.05.

Results and Discussion

Modified T-Junction Design for Production of Larger Microspheroids.

For multiphase microfluidic systems, the control over microspheroid geometry, including AR and diameter, comes from the precise liquid manipulation provided by design of the devices, especially the junction design. There are three commonly used junction designs for microfluidic devices: T-junction, flow focusing, and co-flow. Lach design individually provides different advantages for controlling microspheroid size and AR during the production process. Flow ratio, the ratio of discrete phase to continuous phase flow, is known to play an important role in geometric control. Varying the flow ratio in a T-junction device tends to be more easily used to

adjust the microspheroid AR than their diameter.²⁵ In contrast for flow focusing and co-flow junction designs, although it is also possible to control the AR,²⁶⁻²⁷ changing the flow ratio is more likely to influence the final microspheroid diameter.²⁸⁻²⁹ Due to the complex and resource-intensive nature of traditional microfluidic device fabrication, computational simulation has previously been done for a range of junction designs to provide researchers with a better understanding of the mechanisms controlling microspheroid geometries.²⁹⁻³¹

These experimentally and computationally identified relationships for small microspheroids (produced with traditional PDMS and capillary microfluidic devices) were not able to be replicated, however, for microfluidic production of larger microspheroids. Through numerous "trial and error" design iterations, we established a microfluidic system that could produce larger microspheroids with different diameters for cell encapsulation.²³ However, to systemically control the geometric shape, we needed to establish an understanding of the key design attributes involved in this success, especially for the modified T-junction design.

In examining the design of the microfluidic device, the fluid density difference between the aqueous and oil phases was found to play a critical role. Therefore, design components such as vertical device orientation, a flow stabilizer, and a leveled outlet channel were introduced to both exploit and minimize the effect of this density difference. In order to produce large microspheroids and handle high cell concentrations without being clogged, channels with increased diameters are needed. We found that when the large channel microfluidic device is operated horizontally, which is typical for microfluidic systems, the lighter, lower density fluid tends to rise to the top and the heavier, higher density fluid sinks to the bottom when the two phases meet, making the system unstable. The effect of the density difference between the two inlet fluids becomes more substantial as channel size increases. Hence, we designed the microfluidic device to operate vertically instead

of horizontally, exploiting this density difference to assist in microspheroid formation (Figure 1B). The heavier aqueous phase, which is the hydrogel precursor solution, flows into the microfluidic device from the top inlet, and the lighter phase, which is the mineral oil, flows in from the bottom inlet. The upward force resulting from the density difference can then participate in breaking the surface tension of precursor solution, forming droplets at the junction. To prevent the heavier precursor from escaping the aqueous phase and forming unwanted droplets that sink to the bottom inlet prior entering the junction, a restriction segment functioning as a flow stabilizer is introduced (Figure 1C). The authors hypothesize that as the hydrophobic PDMS channel narrows, the capillary effect of the aqueous solution becomes more pronounced, providing stronger cohesion and preventing unwanted droplet escape. Additionally, the flow stabilizer may also drop the pressure of the aqueous solution through a throttling process. The pressure difference at the interface of two phases, which is a driving force causing inter-phase leakage, is then reduced, making it easier to be equalized by surface tension.³² Under the stabilizer is a conical region, which serves to eliminate dead volume of precursor solution. The outlet channel starts with a relatively small diameter at the junction and gradually increases to a constant size. Adjusting the size of this tapered end of outlet channel enables differing flow speed at the junction, providing control over the viscous force in microspheroid formation. Microspheroidal droplets are formed at the junction and are photocrosslinked in the outlet channel. The outlet channel is leveled without tilting up or down to keep the spacing even between droplets, preventing droplets from aggregating owing to gravity.

Unlike PDMS microfluidic devices made using photolithography, this modified T-junction design has larger channels with circular cross-sectional area, which is achieved by the previously reported molding technique, instead of the typical rectangular cross-sectional area.²³ This circular

cross-sectional area is not unique; the Weitz group reported microfluidic devices made with capillary components, which have shown great potential and also can be fabricated by researchers without special photolithography facilities. However, in terms of scalable device fabrication, molding is a well-developed manufacturing process (Figure 1A). Together, with all the design parameters mentioned above, the modified T-junction design makes it possible to produce larger microspheroids with different ARs and sizes.

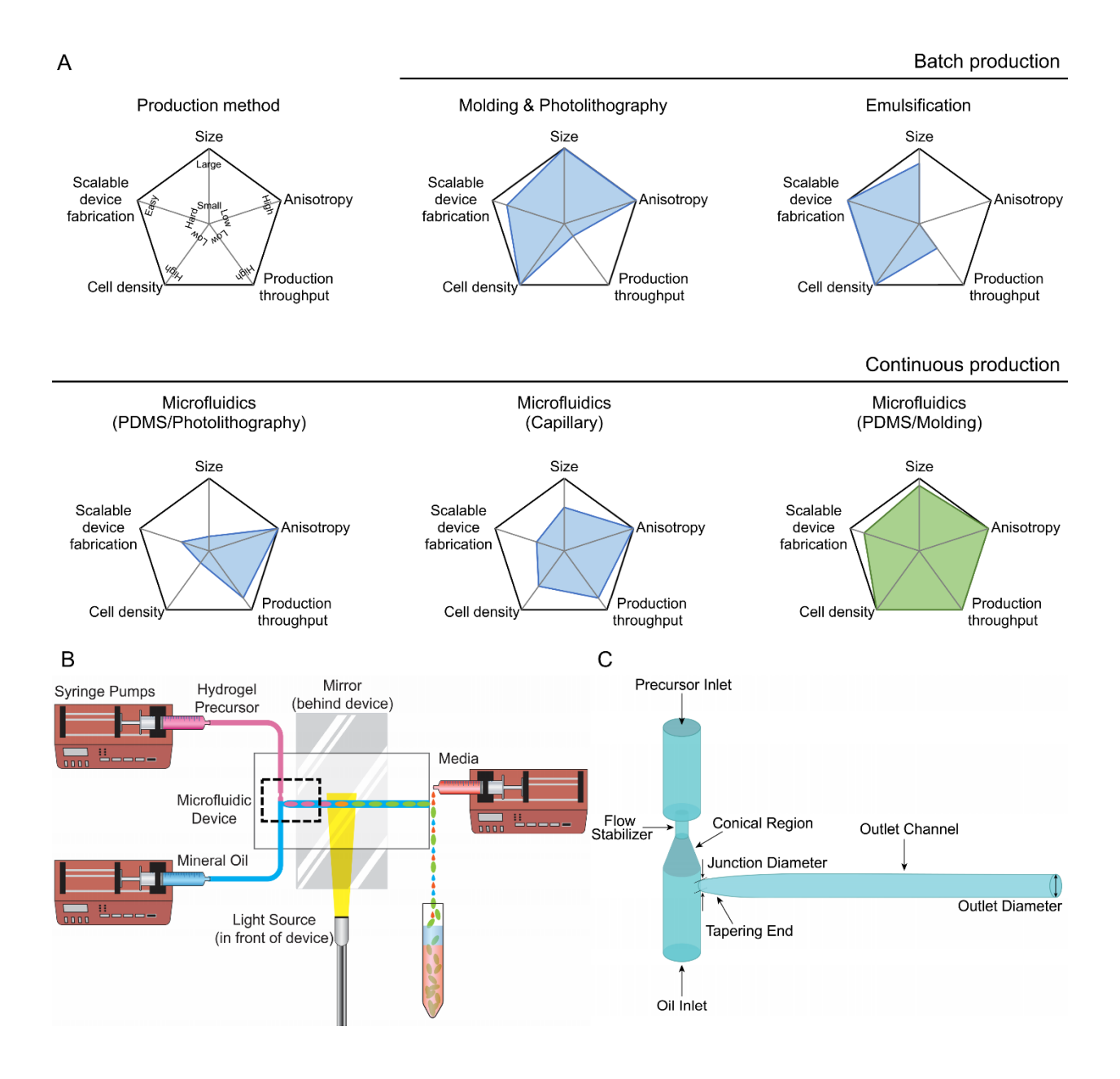


Figure 1. Microfluidic platform with modified T-junction design provides geometric control for large microspheroids. (A) Comparison of capabilities and drawbacks of different methods for producing hydrogel microparticles with controlled geometric shape. Schematic of the (B) microfluidic platform and (C) modified T-junction design.

Production of Uniform Microspheroids with a Wide Range of Geometric Shapes.

In initial testing, this platform using the microfluidic device with modified T-junction design was able to produce uniform hydrogel microspheroids, including microspheres and microrods, with a wide range of geometric shapes. As shown in Figure 2 (A-D), the resulting microspheres had diameters of $320 \pm 10 \mu m$, $590 \pm 20 \mu m$, and $1000 \pm 60 \mu m$ (CV = 0.03, 0.03, and 0.06), respectively. Within the whole diameter range, production of spherical hydrogels is possible with ARs that are close to 1 (1.03 ± 0.02 , 1.02 ± 0.02 , and 1.02 ± 0.02 , respectively), indicating a high degree of roundness. By changing device design parameters and experimental conditions, microspheroids with higher AR, or microrods, were produced. More details are discussed in the following sections. Example microrods are shown in Figure 2 (E-H) with ARs of 1.37 ± 0.04 , 1.98 ± 0.10 , and 3.54 ± 0.37 (CV = 0.03, 0.05, 0.10), respectively.

Previously, microfluidic systems have been widely used to produce microspheres and microrods, ³³⁻³⁴ which have shown great potential for a variety of applications. However, these microfluidic systems would fall short when it comes to cell encapsulation. The microspheres and microrods normally have radial diameters less than 500 μm and therefore can only encapsulate limited numbers of cells, which typically have diameters of 3-50 μm. The microfluidic platform used in this study was able to produce highly uniform microspheroids, similarly to other microfluidic systems, while varying the diameters and ARs at this larger size scale. Each larger

microspheroid individually encapsulates more cells, and the wider range of geometric shapes allows more flexibility in tuning the microenvironment for cells, as well as adjusting the bulk rheological properties of the microspheroid suspension,³⁵ greatly broadening the scope of their functions.

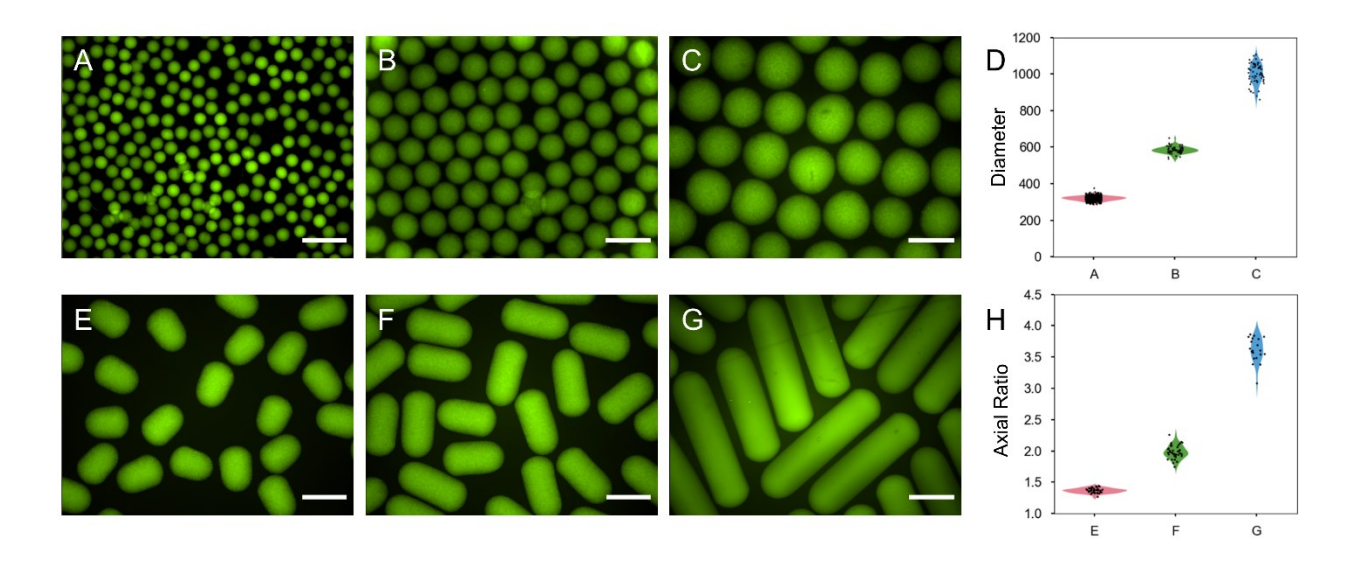


Figure 2. Hydrogel microspheroids with different geometric shapes. (A-C) Imaged by fluorescence microscopy, hydrogel microspheres were shown to have high uniformity, high roundness, and a wide range of diameters (green auto-fluorescence from the photoinitiator Eosin Y used in hydrogel photocrosslinking). (D) Hydrogel microspheres with diameters of $320 \pm 10 \,\mu m$ (CV = 0.03), $590 \pm 20 \,\mu m$ (CV = 0.03), and $1000 \pm 60 \,\mu m$ (CV = 0.06), respectively (n>59 microspheres per condition). (E-G) Hydrogel microrods had high uniformity and a wide range of ARs. (H) Hydrogel microrods with ARs of 1.37 ± 0.04 (CV = 0.03), 1.98 ± 0.10 (CV = 0.05), and 3.54 ± 0.37 (CV = 0.10), respectively (n>20 microrods per condition). Data are presented as mean \pm standard deviation. Scale bar = 1000 μm.

Control Over Geometric Shape Enabled by Modified T-Junction Design.

In modulating the microspheroid geometric shape, the dimensionless capillary number (Ca) plays an important role.³⁶ It describes the relative effect of viscous forces to surface tension at the interface of two immiscible fluids:

$$Ca = \frac{Viscous\ force}{Surface\ tension} = \frac{\mu\nu}{\nu}$$
 (2)

where μ is the dynamic viscosity of continuous phase (oil phase), ν is the relative velocity of continuous phase (oil phase) to discrete phase (aqueous precursor solution) at the junction, and γ is the interfacial tension (precursor solution–oil). The relationship between the microsphere diameter and Ca is described by:

$$Diameter_{Microsphere} \propto \frac{1}{Ca}$$
 (3)

As the Ca increases, the microsphere diameter decreases. As the Ca decreases, the microsphere diameter increases until it is restricted by the outlet channel diameter. Based on the definition of the Ca, as the v increases, the Ca increases. When v decreases, Ca has a lower value. The relative velocity, v, it is related to the flow fraction, which is defined as:

$$Flow Fraction = \frac{Precursor flow rate}{Precursor flow rate + Oil flow rate}$$
(4)

The flow rate is a parameter that can be experimentally controlled; therefore, by adjusting the flow rate, we can control the v and Ca, eventually controlling the resulting diameter of microspheres. As the microsphere diameter increases and becomes larger than outlet channel diameter, the droplets elongate and become microrods because of the constraints from the outlet channel wall.

When using a light source with consistent power output, exposure time plays an important role in controlling degree of photocrosslinking, which can be reflected in hydrogel stiffness.³⁷ Therefore, to ensure consistent photocrosslinking in our platform, the microspheroids must have similar exposure time to the visible light source when traveling through the outlet channel, which means they need to have a similar flow velocity in the outlet channel. Flow velocity is defined by volumetric flow rate, controlled by the syringe pumps, over cross-sectional area of the microfluidic device outlet channel, which is proportional to the square of outlet channel diameter.

Using this relationship, the total volumetric flow rate was adjusted based on the outlet channel diameter to maintain a similar velocity in the outlet channel, providing consistent microspheroid crosslinking times. As a result, the ν is determined not only by the diameter of the junction, but also by the diameter of the outlet channel. For example, for two microfluidic devices with the same junction diameter, the one with a larger outlet channel diameter requires a higher volumetric flow rate to achieve the same velocity in outlet channel, resulting with a higher velocity at the junction.

To better account for the impact of v on microspheroid geometry in our system, we introduce a dimensionless parameter, Narrowing Ratio (NR), to describe the relative size of junction diameter and outlet channel diameter. The NR determines the v while also accounting for the velocity in the outlet channel as shown in Supporting Information (S3). Therefore, controlling NR provides control over Ca, which regulates the tendency of a microfluidic device to produce microspheres or microrods:

$$Narrowing \ Ratio(NR) = \frac{Diameter_{Junction}}{Diameter_{Outlet}}$$
 (5)

For devices with the same outlet channel diameter, the total volumetric flow rate needs to be held constant to ensure similar flow velocity in the outlet channel, which is important for controlling degree of photocrosslinking as discussed previously. Therefore, as the NR is decreased, the junction diameter also decreases, leading to a smaller cross-sectional area at the junction. As a result, the v goes up, which means Ca is also higher. Similarly, as the NR is increased, the v goes down, decreasing the Ca (Figure 3).

Using these relationships, we found that the NR in combination with flow fraction could be used to control microspheroid geometry in our microfluidic platform. Through experimental observations, we determined that when the NR value was smaller than 0.5, the shape of the resulting droplets was typically spherical, and the size depended on flow fraction. As the flow fraction was increased, the diameter of the microspheres also increased until reaching the diameter of the outlet channel. Further increase in the flow fraction then resulted in higher numbers of microspheroids per time being generated at the junction. In contrast, when the NR value was larger than 0.5, microspheroid radial diameter was not dependent on flow fraction; instead, the shape of the resulting droplets could be changed from microsphere to microrod depending on the flow fraction, and the radial diameter depended on outlet channel diameter. When the flow fraction was increased, the microspheroids AR increased. The use of these identified relationships to control microspheroid size and geometry is summarized in Figure 3.

Although Reynolds number potentially provides another metric for comparison between this system and other microfluidic platforms, it was not a particularly useful parameter in predicting geometric shapes in our microfluidic system (detailed justification provided in Supporting Information S4). Collectively, here we found that by adjusting design parameters including junction diameter and outlet channel diameter, and experimental parameters such as the inlet flow

rates of the precursor solution and mineral oil, the geometric shape of microspheroids can be adjusted. Future work will further investigate these identified relationships, as well as consider the potential influence of transition length at the tapered end of the outlet channel.

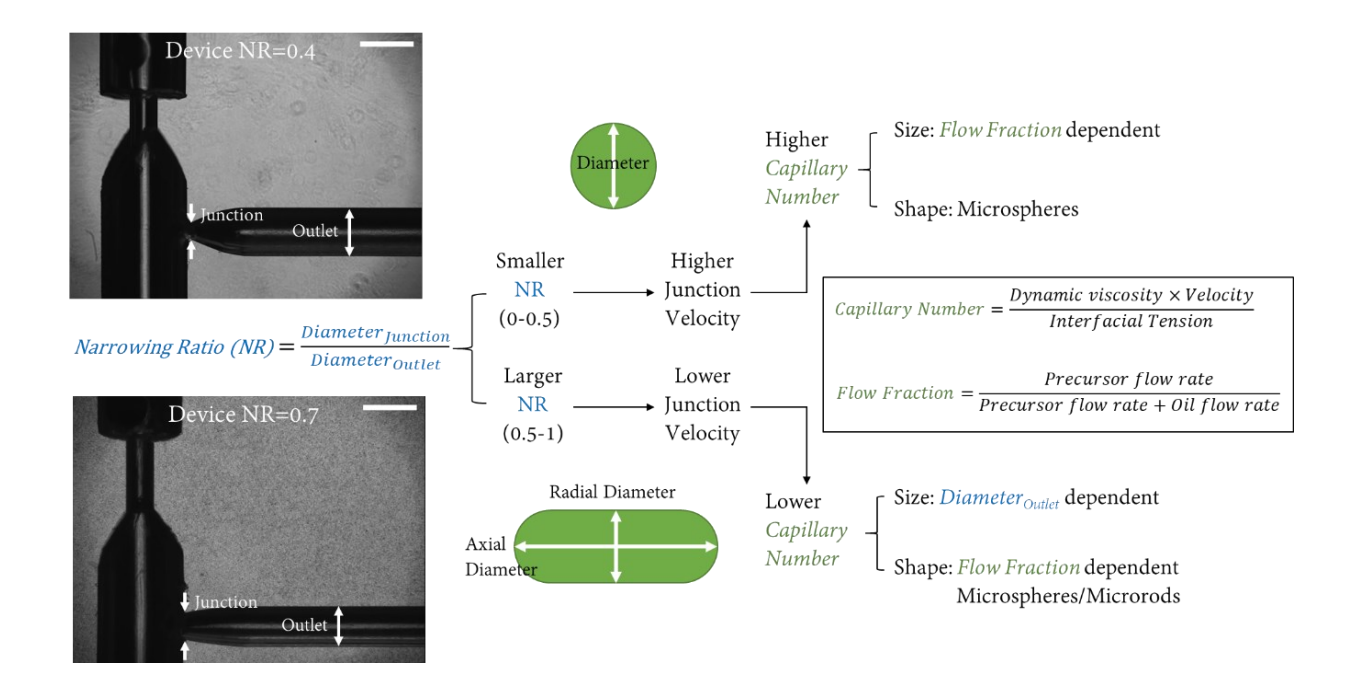


Figure 3. A summary of governing fundamental physical principles for the modified T-junction. By adjusting design parameters such as junction diameter and outlet diameter and experimental parameters such as inlet flow rates of precursor and oil, we can control the capillary number at the junction. As a result, the size and shape of microspheroids can be adjusted. Images of microfluidic device were modified for better visualization, and original images were shown in Figure S1 (Supporting Information S5).

Control of Geometric Shape by Varying Narrowing Ratio and Flow Fraction.

To demonstrate the relationships summarized in the previous section, microfluidic devices with two different NRs (0.4 and 0.7) were fabricated and operated with different flow fractions. The microfluidic device with NR = 0.4 produced spherical hydrogels (Figure 4A-C). When increasing the flow fraction from 0.05 to 0.07, the microsphere diameter increased significantly from $680 \pm 10~\mu m$ to $930 \pm 20~\mu m$ (Figure 4D). The resulting diameter stopped increasing with subsequent increases to flow fraction once the microspheres reached the size of the outlet channel. For the microfluidic device with NR = 0.7, the microspheroid radial diameter was limited to the outlet channel diameter, approximately 800 μm . With an increase of flow fraction from 0.1 to 0.7, the axial diameter increased significantly from $820 \pm 20~\mu m$ to $3010 \pm 170~\mu m$, leading to a significant increase of AR from 1.02 ± 0.01 to 3.61 ± 0.20 (Figure 4E-I). Detailed information on device design parameters and experimental conditions is listed in Table 1. These results demonstrate that this microfluidic device provides tight control over microspheroid geometric shape by varying the NR and flow fraction.

These general relationships to guide device design, including investigation of flow fraction, narrowing ratio, and capillary number dimensionless parameters, have been used to successfully design numerous additional large channel microfluidic devices, examples of which are provided in Supporting Information (Table S1, current list of tested designs available upon request). These parameters provide a basis for extension of geometric control to other large dimension microfluidic platforms.

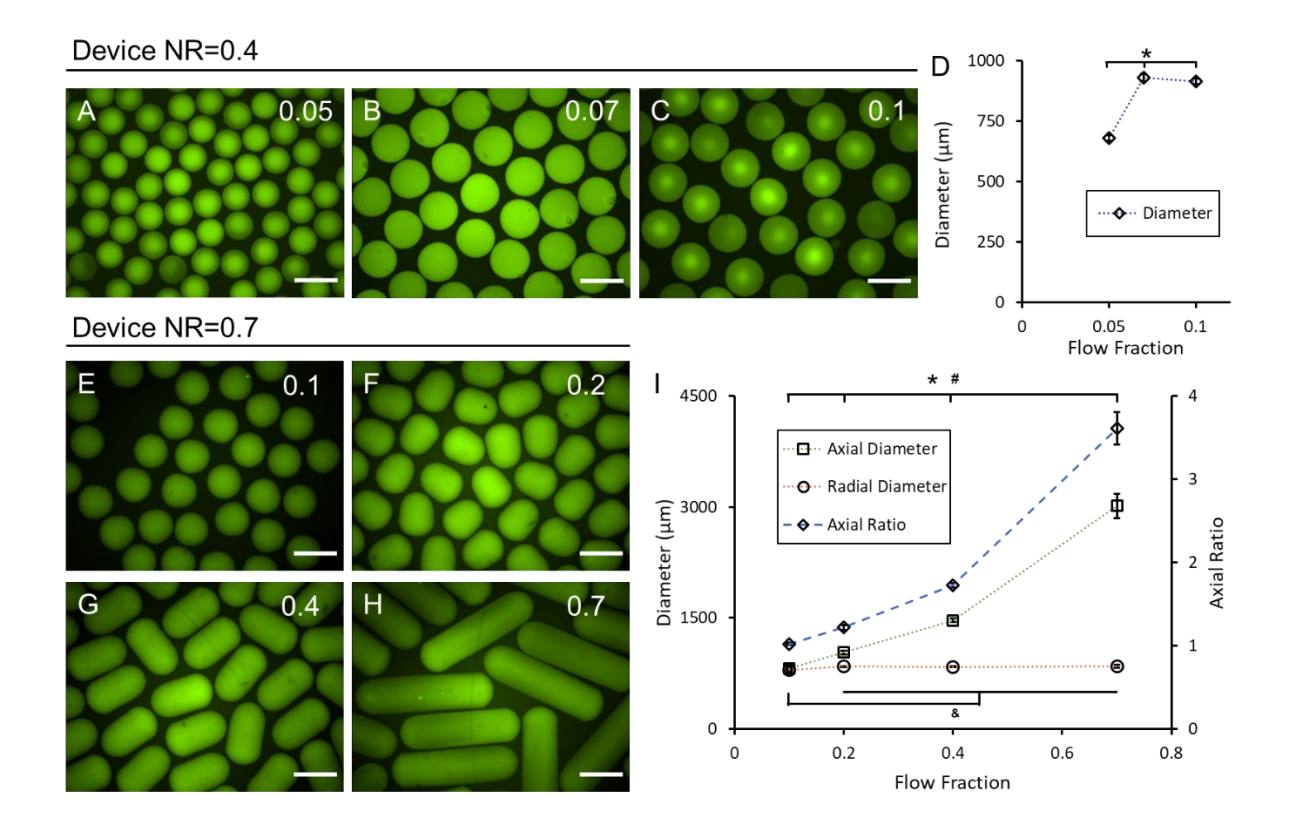


Figure 4. The microfluidic device provides tight control over the microspheroid geometric shape by varying the NR and flow fraction. (A-C) A microfluidic device with a small NR (NR = 0.4) produced microspheres. The diameter of microspheres changed with flow fraction. (D) When the NR = 0.4, quantitative analysis showed microsphere diameter increased with flow fraction and then stopped upon reaching the size of the outlet channel (*Significant difference between flow fractions for diameter, p<0.05, n>70 microspheroids per condition). (E-H) A microfluidic device with a large NR (NR = 0.7) produced both microspheres and microrods. By increasing the flow fraction, the radial diameter remained relatively constant while the axial diameter increased, causing an increase in AR. (I) When NR = 0.7, quantitative analysis showed microrod AR increased along with flow fraction (*****Significant difference between flow fractions for AR, axial diameter, and radial diameter, respectively, p<0.05, n>20 microspheroids per condition). Data are presented as mean ± standard deviation. Scale bar = 1000 μm.

Table 1. Microfluidic device design parameters and experimental conditions for production of microspheroids shown in Figure 4.

Device	NR=0.4			NR=0.7			
Junction Size (μm)	370			530			
Outlet Size (µm)	920			770			
Flow Fraction	0.05	0.07	0.1	0.1	0.2	0.4	0.7
Oil Flow Rate (mL/hr)	10	10	9	9	8	6	3
Precursor Flow Rate (mL/hr)	0.5	0.8	1	1	2	4	7
Axial Diameter (µm)	680 ± 10	930 ± 20	920 ± 10	820 ± 20	1040 ± 30	1470 ± 20	3010 ± 170
Radial Diameter (µm)	660 ± 10	910 ± 20	890 ± 10	800 ± 20	840 ± 10	840 ± 10	850 ± 20
Axial Ratio (AR)	1.01 ± 0.01	1.01 ± 0.01	1.01 ± 0.01	1.02 ± 0.01	1.22 ± 0.03	1.72 ± 0.03	3.61 ± 0.20

Note: For microspheres (AR < 1.05), the diameter reported in the text is always the axial diameter.

Cell-Laden Microspheroids for Biomedical Applications

Different types of cells were successfully encapsulated in anisotropic hydrogel microspheroids, including human BJ-5ta fibroblasts and equine ECFCs. BJ-5ta fibroblasts were encapsulated in microspheroids (13 million cells/mL) with different ARs. Geometric shape of microspheroids and viability of encapsulated cells were observed one day after encapsulation for both qualitative and quantitative assessment. As shown in Figure 5A, the fibroblast-laden microspheroids from both groups were highly uniform with even cell distribution. The AR for each group was 1.37 ± 0.04 and 1.98 ± 0.10 , respectively (Figure 5B). Encapsulated cells maintained high viability (>93% for both groups) after encapsulation (Figure 5A, C). The cells formed an actin filament network as shown in Figure 5A. These results show that the microfluidic platform can provide control over ARs during the cell-laden microspheroid production process. The encapsulated fibroblasts maintained high viability and normal cellular activities.

ECFC-laden hydrogel microrods were produced (Figure 5D) with axial diameter of 3490 \pm 170 μ m (CV = 0.05) and radial diameter of 770 \pm 20 μ m (CV = 0.02) (Figure 5E), leading to an AR of 4.79 \pm 0.27 (CV = 0.06). Encapsulated cells maintained high viability and elongated to form web-like cell-cell interactions within the hydrogel microspheroids by day 7 of culture (Figure 5F). Since the hydrogels were formed using PEG-fibrinogen, which contains enzymatic cleavage sites, ³⁸ the microspheroids can be degraded and remodeled by the encapsulated cells. As reported in our previous work, the ECFCs were expected to remodel their surrounding environment, altering the mechanical properties of the hydrogels. ^{4, 23} Based on direct visual observation, the number of cells within the hydrogels was found to increase along with time, indicating the proliferation of the ECFCs. In addition, initial cell-cell interactions were observed in between hydrogels (Figure 5G, yellow arrows). These inter-hydrogel interactions increased as the ECFCs actively proliferated and migrated, pulling multiple hydrogels together to form even larger tissues with more complex structures as seen at day 12 (Figure 5H). In comparison, inter-hydrogel interactions were not seen between acellular microspheroids.

Fabrication of macroscopic tissues using microscopic cell-laden hydrogels as the building blocks has attracted much attention.^{7-8, 39-40} Anisotropic microspheroids can be used for culturing cells that are sensitive to spatial heterogeneity such as aligning cardiomyocytes and neurons to promote functional development of engineered cardiac or neural tissues.⁴¹⁻⁴² With larger sizes, the hydrogels can encapsulate more cells and be more efficient in building macroscopic tissues. Future work will investigate this approach to direct the assembly of anisotropic microspheroids, controlling the structure and complexity of the macrotissues, such as has been established previously for smaller microspheroids.⁸

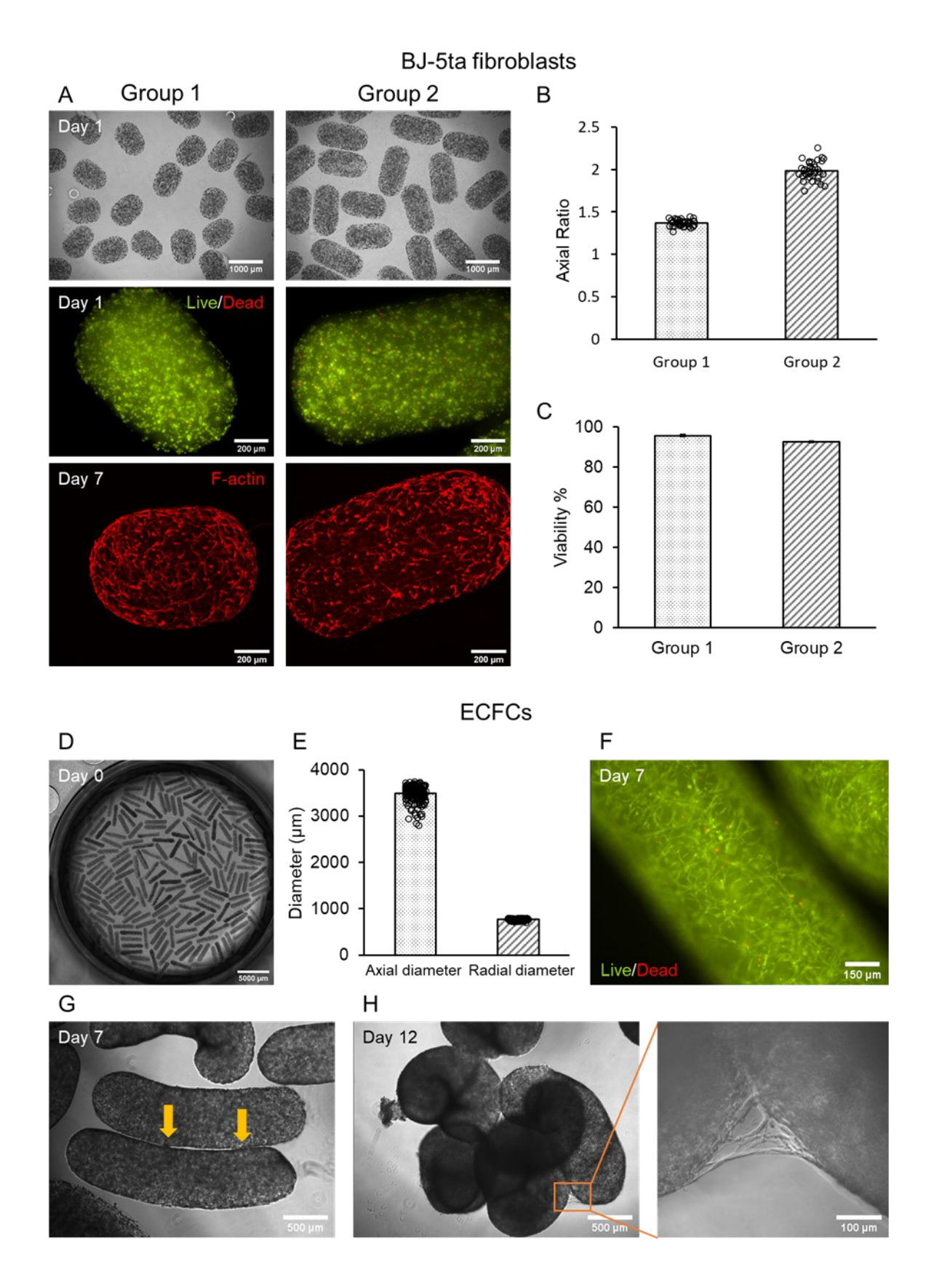


Figure 5. Cell-laden microspheroids with different ARs supported normal cellular activities post-encapsulation. (A) Fibroblast-laden microspheroids had uniform geometric shape and even cell distribution visualized using phase contrast images. Encapsulated cells maintained high viability after encapsulation and formed an actin filament network shown by fluorescence images. (B) Fibroblast-laden microspheroids had ARs of 1.37 \pm 0.04 (CV = 0.03) and 1.98 \pm 0.10 (CV = 0.05), respectively, for each group one day after encapsulation (n > 37 microspheroids per group). (C) Encapsulated fibroblasts maintained high viability of 96 ± 1 and 93 ± 1 percent, respectively, for each group one day after encapsulation (n = 3 microspheroids per group). (D) ECFC-laden microspheroids had uniform geometric shape and even cell distribution as visualized using phase contrast microscopy. (E) ECFC-laden microspheroids had an axial diameter of 3490 ± 170 µm (CV = 0.05) and a radial diameter of 770 \pm 20 μ m (CV = 0.02). (F) Encapsulated ECFCs maintained high viability and elongated to form web-like cell-cell interactions within the hydrogel microspheroids by day 7 of culture. (G) Initial cell-cell interactions were observed between hydrogels as indicated by yellow arrows at day 7. (H) Macroscopic tissue formed by ECFC-laden microspheroids at day 12. Cell-cell connections between microspheroids can be seen in the enlarged picture.

Geometric shape of microspheroids directly impacts their performance. Control over the diameters and ARs of microspheroids opens many exciting possibilities for various applications. Currently a number of approaches have been developed to vary geometric shape from the microscale down to nanoscale, such as molding,⁴³ emulsion,¹² electrospray,⁴⁴ and microfluidic techniques.³⁴ Compared to other methods, microfluidics can provide higher uniformity and production throughput.³ However, most research using microfluidics to achieve geometric shape control is done utilizing small channel sizes.²⁰ Whereas the resulting small microspheroids are

necessary for purposes such as drug delivery, the low upper size constraint limits their use in many other applications. Here we described a microfluidic platform with a modified T-junction design that can control the diameters and ARs of microspheroids with larger sizes (on the dimensions of hundreds to thousands of microns). We also identified and examined the mechanisms by which this junction design provides geometric control, including the role of narrowing ratio, capillary number and flow fraction. Findings from this work provide an approach for rapid production of cell-laden hydrogels with controlled geometric shapes, clearing the path for further investigation of geometric shape-related biomedical applications.

Conclusion

In conclusion, here we demonstrated the ability to produce hydrogel microspheroids, including microspheres and microrods, using our microfluidic platform. The PDMS microfluidic device used in this platform employed a modified T-junction fabricated with a molding technique.²³ This special junction design enabled production of uniform microspheroids with larger sizes than typically achieved with microfluidic systems and a wide range of ARs. We explored the mechanisms by which the junction design facilitates large microspheroid formation and provides control over the geometric shape. We show that by varying the design (narrowing ratio) and experimental (flow fraction) parameters, we can control whether the microfluidic device produces microspheres or microrods and adjust their diameters and ARs. To demonstrate the potential of the microspheroids for use in biomedical applications, we encapsulated fibroblasts within the hydrogel microspheroids with controlled ARs and have shown continued normal cellular behavior as well as high viability during culture. In addition, ECFC-laden microspheroids were produced and demonstrated the potential to self-assemble into macroscopic tissues. With the increased

understanding of the governing principles determined here from both literature and experiment, this microfluidic platform provides opportunities for scalable production of large cell-laden microspheroids with desired geometric shape for various applications, such as bioreactor-based cell production, injectable cell delivery, disease modeling for drug discovery, and 3D bioprinting.

ASSOCIATED CONTENT

Supporting Information.

PEGDA and PEG-fibrinogen synthesis. Microfluidic device fabrication and microfluidic platform setup. Regulation of relative velocity by narrowing ratio (NR). Justification for not using Reynolds number as a parameter for predicting geometric shape in our microfluidic device. The original images of T-junction in microfluidic device designs. Examples of microfluidic device designs.

AUTHOR INFORMATION

Author Contributions

The manuscript was written through contributions of all authors. All authors have given approval to the final version of the manuscript.

Notes

Auburn University has one patent application submitted for the microfluidic cell encapsulation system employed. 1. EA Lipke, Y Tian*, WJ Seeto*, "Microfluidics Device for Fabrication of Large, Uniform, Injectable Hydrogel Microspheres for Cell Encapsulation." Provisional Patent 62/568,652, filed 10/6/2017. US Patent Application No. 16/153,095, filed 10/5/2018, published, pending.

ACKNOWLEDGMENT

This work was funded by the National Science Foundation (NSF-CBET- 1743445) (Y.T. and E.A.L.), the American Heart Association (AM HEART-14SDG18610002) (Y.T. and E.A.L.), and the Alabama EPSCoR Graduate Research Scholarship Program (Y.T.).

ABBREVIATIONS

ANOVA, analysis of variance; AR, axial ratio; Ca, capillary number; DMEM, Dulbecco's Modified Eagle's Medium; ECFC, endothelial colony forming cells; FBS, fetal bovine serum; NR, narrowing ratio; PDMS, polydimethylsiloxane; PEG-fibrinogen, poly(ethylene glycol)-fibrinogen

REFERENCES

- 1. de Vicente, J.; Segovia-Gutierrez, J. P.; Andablo-Reyes, E.; Vereda, F.; Hidalgo-Alvarez, R., Dynamic rheology of sphere- and rod-based magnetorheological fluids. *J Chem Phys* **2009**, *131* (19), 194902.
- 2. Champion, J. A.; Mitragotri, S., Role of target geometry in phagocytosis. *Proc Natl Acad Sci U S A* **2006**, *103* (13), 4930-4.
- 3. Khademhosseini, A.; Langer, R., Microengineered hydrogels for tissue engineering. *Biomaterials* **2007**, *28* (34), 5087-92.
- 4. Seeto, W. J.; Tian, Y.; Winter, R. L.; Caldwell, F. J.; Wooldridge, A. A.; Lipke, E. A., Encapsulation of Equine Endothelial Colony Forming Cells in Highly Uniform, Injectable Hydrogel Microspheres for Local Cell Delivery. *Tissue Eng Part C Methods* **2017**, *23* (11), 815-825.
- 5. Kropp, C.; Massai, D.; Zweigerdt, R., Progress and challenges in large-scale expansion of human pluripotent stem cells. *Process Biochemistry* **2017**, *59*, 244-254.
- 6. Zhu, Z.; Yang, C. Y. J., Hydrogel Droplet Microfluidics for High-Throughput Single Molecule/Cell Analysis. *Accounts of Chemical Research* **2017**, *50* (1), 22-31.
- 7. Highley, C. B.; Song, K. H.; Daly, A. C.; Burdick, J. A., Jammed Microgel Inks for 3D Printing Applications. *Adv Sci (Weinh)* **2019**, *6* (1), 1801076.
- 8. Ma, S. H.; Mukherjee, N.; Mikhailova, E.; Bayley, H., Gel Microrods for 3D Tissue Printing. *Advanced Biosystems* **2017**, *I* (8).
- 9. Zhao, X.; Liu, S.; Yildirimer, L.; Zhao, H.; Ding, R. H.; Wang, H. N.; Cui, W. G.; Weitz, D., Injectable Stem Cell-Laden Photocrosslinkable Microspheres Fabricated Using Microfluidics for Rapid Generation of Osteogenic Tissue Constructs. *Advanced Functional Materials* **2016**, *26* (17), 2809-2819.
- 10. Oliveira, M. B.; Kossover, O.; Mano, J. F.; Seliktar, D., Injectable PEGylated fibrinogen cell-laden microparticles made with a continuous solvent- and oil-free preparation method. *Acta Biomater* **2015**, *13*, 78-87.
- 11. Yao, R.; Zhang, R.; Lin, F.; Luan, J., Biomimetic injectable HUVEC-adipocytes/collagen/alginate microsphere co-cultures for adipose tissue engineering. *Biotechnol Bioeng* **2013**, *110* (5), 1430-43.
- 12. Franco, C. L.; Price, J.; West, J. L., Development and optimization of a dual-photoinitiator, emulsion-based technique for rapid generation of cell-laden hydrogel microspheres. *Acta Biomater* **2011**, *7* (9), 3267-76.
- 13. Dendukuri, D.; Gu, S. S.; Pregibon, D. C.; Hatton, T. A.; Doyle, P. S., Stop-flow lithography in a microfluidic device. *Lab on a Chip* **2007**, *7* (7), 818-828.
- 14. Christopher, G. F.; Anna, S. L., Microfluidic methods for generating continuous droplet streams. *Journal of Physics D-Applied Physics* **2007**, *40* (19), R319-R336.

- 15. Xu, Q.; Hashimoto, M.; Dang, T. T.; Hoare, T.; Kohane, D. S.; Whitesides, G. M.; Langer, R.; Anderson, D. G., Preparation of monodisperse biodegradable polymer microparticles using a microfluidic flow-focusing device for controlled drug delivery. *Small* **2009**, *5* (13), 1575-81.
- 16. Hindson, B. J.; Ness, K. D.; Masquelier, D. A.; Belgrader, P.; Heredia, N. J.; Makarewicz, A. J.; Bright, I. J.; Lucero, M. Y.; Hiddessen, A. L.; Legler, T. C.; Kitano, T. K.; Hodel, M. R.; Petersen, J. F.; Wyatt, P. W.; Steenblock, E. R.; Shah, P. H.; Bousse, L. J.; Troup, C. B.; Mellen, J. C.; Wittmann, D. K.; Erndt, N. G.; Cauley, T. H.; Koehler, R. T.; So, A. P.; Dube, S.; Rose, K. A.; Montesclaros, L.; Wang, S.; Stumbo, D. P.; Hodges, S. P.; Romine, S.; Milanovich, F. P.; White, H. E.; Regan, J. F.; Karlin-Neumann, G. A.; Hindson, C. M.; Saxonov, S.; Colston, B. W., High-throughput droplet digital PCR system for absolute quantitation of DNA copy number. *Anal Chem* **2011**, *83* (22), 8604-10.
- 17. Choi, C. H.; Wang, H.; Lee, H.; Kim, J. H.; Zhang, L.; Mao, A.; Mooney, D. J.; Weitz, D. A., One-step generation of cell-laden microgels using double emulsion drops with a sacrificial ultra-thin oil shell. *Lab Chip* **2016**, *16* (9), 1549-55.
- 18. Utada, A. S.; Lorenceau, E.; Link, D. R.; Kaplan, P. D.; Stone, H. A.; Weitz, D. A., Monodisperse double emulsions generated from a microcapillary device. *Science* **2005**, *308* (5721), 537-41.
- 19. Othman, R.; Vladisavljević, G. T.; Nagy, Z. K., Preparation of biodegradable polymeric nanoparticles for pharmaceutical applications using glass capillary microfluidics. *Chemical Engineering Science* **2015**, *137*, 119-130.
- 20. Velasco, D.; Tumarkin, E.; Kumacheva, E., Microfluidic encapsulation of cells in polymer microgels. *Small* **2012**, *8* (11), 1633-42.
- 21. Kruger, A. J. D.; Bakirman, O.; Guerzoni, L. P. B.; Jans, A.; Gehlen, D. B.; Rommel, D.; Haraszti, T.; Kuehne, A. J. C.; De Laporte, L., Compartmentalized Jet Polymerization as a High-Resolution Process to Continuously Produce Anisometric Microgel Rods with Adjustable Size and Stiffness. *Adv Mater* **2019**, *31* (49), e1903668.
- 22. Pradhan, S.; Chaudhury, C. S.; Lipke, E. A., Dual-phase, surface tension-based fabrication method for generation of tumor millibeads. *Langmuir* **2014**, *30* (13), 3817-25.
- 23. Seeto, W. J.; Tian, Y.; Pradhan, S.; Kerscher, P.; Lipke, E. A., Rapid Production of Cell-Laden Microspheres Using a Flexible Microfluidic Encapsulation Platform. *Small* **2019**, e1902058.
- 24. Sharpe, A. N.; Seeto, W. J.; Winter, R. L.; Zhong, Q.; Lipke, E. A.; Wooldridge, A. A., Isolation of endothelial colony-forming cells from blood samples collected from the jugular and cephalic veins of healthy adult horses. *Am J Vet Res* **2016**, *77* (10), 1157-65.
- 25. Tice, J. D.; Song, H.; Lyon, A. D.; Ismagilov, R. F., Formation of droplets and mixing in multiphase microfluidics at low values of the Reynolds and the capillary numbers. *Langmuir* **2003**, *19* (22), 9127-9133.
- 26. Cheng, Y.; Zhu, C.; Xie, Z. Y.; Gu, H. C.; Tian, T.; Zhao, Y. J.; Gu, Z. Z., Anisotropic colloidal crystal particles from microfluidics. *Journal of Colloid and Interface Science* **2014**, *421*, 64-70.
- 27. Jiang, Z.; Shaha, R.; McBride, R.; Jiang, K.; Tang, M.; Xu, B.; Goroncy, A. K.; Frick, C.; Oakey, J., Crosslinker length dictates step-growth hydrogel network formation dynamics and allows rapid on-chip photoencapsulation. *Biofabrication* **2020**, *12* (3), 035006.
- 28. Anna, S. L.; Bontoux, N.; Stone, H. A., Formation of dispersions using "flow focusing" in microchannels. *Applied Physics Letters* **2003**, *82* (3), 364-366.

- 29. Hong, Y. P.; Wang, F. J., Flow rate effect on droplet control in a co-flowing microfluidic device. *Microfluidics and Nanofluidics* **2007**, *3* (3), 341-346.
- 30. Dupin, M. M.; Halliday, I.; Care, C. M., Simulation of a microfluidic flow-focusing device. *Physical Review E* **2006**, *73* (5).
- 31. Liu, H. H.; Zhang, Y. H., Droplet formation in a T-shaped microfluidic junction. *Journal of Applied Physics* **2009**, *106* (3).
- 32. Aota, A.; Hibara, A.; Kitamori, T., Pressure balance at the liquid-liquid interface of micro countercurrent flows in microchips. *Analytical Chemistry* **2007**, *79* (10), 3919-3924.
- 33. Wan, J. D.; Shi, L.; Benson, B.; Bruzek, M. J.; Anthony, J. E.; Sinko, P. J.; Prudhomme, R. K.; Stone, H. A., Microfluidic Generation of Droplets with a High Loading of Nanoparticles. *Langmuir* **2012**, *28* (37), 13143-13148.
- 34. Seemann, R.; Brinkmann, M.; Pfohl, T.; Herminghaus, S., Droplet based microfluidics. *Rep Prog Phys* **2012**, *75* (1), 016601.
- 35. Mueller, S.; Llewellin, E.; Mader, H. J. P. o. t. R. S. A. M., Physical; Sciences, E., The rheology of suspensions of solid particles. **2010**, *466* (2116), 1201-1228.
- 36. Xu, J. H.; Li, S. W.; Tan, J.; Wang, Y. J.; Luo, G. S., Preparation of highly monodisperse droplet in a T-junction microfluidic device. *Aiche Journal* **2006**, *52* (9), 3005-3010.
- 37. Bonino, C. A.; Samorezov, J. E.; Jeon, O.; Alsberg, E.; Khan, S. A., Real-time in situ rheology of alginate hydrogel photocrosslinking. *Soft Matter* **2011**, *7* (24), 11510-11517.
- 38. Almany, L.; Seliktar, D., Biosynthetic hydrogel scaffolds made from fibrinogen and polyethylene glycol for 3D cell cultures. *Biomaterials* **2005**, *26* (15), 2467-77.
- 39. Du, Y.; Lo, E.; Ali, S.; Khademhosseini, A., Directed assembly of cell-laden microgels for fabrication of 3D tissue constructs. *Proc Natl Acad Sci U S A* **2008**, *105* (28), 9522-7.
- 40. Xin, S.; Chimene, D.; Garza, J. E.; Gaharwar, A. K.; Alge, D. L., Clickable PEG hydrogel microspheres as building blocks for 3D bioprinting. *Biomater Sci* **2019**, *7* (3), 1179-1187.
- 41. McCain, M. L.; Agarwal, A.; Nesmith, H. W.; Nesmith, A. P.; Parker, K. K., Micromolded gelatin hydrogels for extended culture of engineered cardiac tissues. *Biomaterials* **2014**, *35* (21), 5462-71.
- 42. Shepherd, J. N. H.; Parker, S. T.; Shepherd, R. F.; Gillette, M. U.; Lewis, J. A.; Nuzzo, R. G., 3D Microperiodic Hydrogel Scaffolds for Robust Neuronal Cultures. *Advanced Functional Materials* **2011**, *21* (1), 47-54.
- 43. Rolland, J. P.; Maynor, B. W.; Euliss, L. E.; Exner, A. E.; Denison, G. M.; DeSimone, J. M., Direct fabrication and harvesting of monodisperse, shape-specific nanobiomaterials. *J Am Chem Soc* **2005**, *127* (28), 10096-100.
- 44. Jaworek, A., Electrospray droplet sources for thin film deposition. *Journal of Materials Science* **2007**, *42* (1), 266-297.

For Table of Contents Use Only

Microfluidic Production of Cell-Laden Microspheroidal Hydrogels with Different Geometric Shapes

Yuan Tian, Elizabeth A. Lipke

